Online Repository Materials

Neonatal rhinovirus induces mucous metaplasia and airways hyperresponsiveness via IL-25 and ILC2s

Methods

Generation of RV. RV1B (ATCC, Manassas, VA) were grown in HeLa cells, concentrated and partially purified [1]. Similarly concentrated and purified HeLa cell lysates were used for sham infection. Viral titer was measured by fifty percent tissue culture infectivity doses ($TCID_{50}$) using the Spearman-Karber method [2] or by plaque assay [3]. For the plaque assay, HeLa cell monolayers were infected with serially-diluted RV and overlayed with a 0.6% agarose solution. Plaque growth was monitored by light microscopy and was confirmed by staining with crystal violet.

Assessment of airway responsiveness. Airway cholinergic responsiveness was assessed by measuring changes in total respiratory system resistance in response to increasing doses of nebulized methacholine [4]. Mice were anesthetized with sodium pentobarbital (50 mg/kg mouse, intraperitoneal injection) and a tracheostomy performed. Mechanical ventilation was conducted and total respiratory system measured using a Buxco FinePointe operating system (Buxco, Wilmington, NC). Airway responsiveness was assessed by measuring changes in resistance in response to increasing doses of nebulized methacholine. Statistical analysis was performed using two-way ANOVA with repeated measures, employing Graph Pad Prism 6.0 software program.

Histology and immunohistochemistry. Lungs were collected and fixed with 10% formaldehyde and paraffin embedded. Blocks were sectioned at 500-μm intervals at a thickness of 5 μm, and each section was deparaffinized and hydrated. After antigen demasking and permeabilization, sections were incubated with Alexa Fluor (AF)-488-conjugated rabbit anti-mouse IL-25/IL-17E (Millipore, Billerica, MA), guinea pig antiserum against HRV1B (ATCC), or AF-conjugated isotype control IgGs. Antiserum was partially purified by incubation with nitrocellulose-bound HeLa cell proteins and passing through an affinity resin containing nondenatured mouse lung protein, as described previously [5]. Repurified antibody was directly conjugated to AF594. The control used was AF594-conjugated guinea pig antiserum. Nuclei

were stained with 4′,6-diamidino-2-phenylindole. Images were visualized using a Zeiss Axioplan microscope equipped with an ApoTome and digital AxioCamMR charge-coupled device camera. To visualize mucus, deparaffinized sections were stained with periodic acid-Schiff (Sigma-Aldrich, St. Louis, MO).

Measurement of IL-13 and IL-25. IL-13 and IL-25 concentrations were measured with ELISA (eBioscience, San Diego, CA). The amount of IL-25 per lung weight was calculated by multiplying the concentration by the volume of lung homogenate divided by the weight of lungs.

Real-time quantitative PCR. Lung RNA was extracted with Trizol method (Invitrogen, Carlsbad, CA) with the combination of on-column digestion of genomic DNA (Qiagen, Valencia, CA). cDNA was synthesized from 1 μg of RNA and subjected to quantitative real-time PCR using specific mRNA primers for IL-4, IL-5, IL-13, IFN-γ, IL-12p40, TNF-α, Muc5ac, Muc5b, Gob5 and IL-17RB. The sequences of specific primers are provided (Supplemental Table E1).The level of gene expression was normalized to mRNA of GAPDH.

Flow cytometric analysis. Lungs were perfused with PBS containing EDTA, minced and digested in collagenase IV. Cells were filtered and washed with RBC lysis buffer, and dead cells were stained with Pac-Orange Live/Dead fixable dead staining dye (Invitrogen, Carlsbad, CA). Lung cells were then stained with FITC-conjugated antibodies for lineage markers (CD3ε, TCRβ, B220/CD45R, Ter-119, Gr-1/Ly-6G/Ly-6C, CD11b, CD11c, F4/80 and FcεRIα, from Biolegend), anti-CD25-PerCP-Cy5.5 (Biolegend), anti-CD127-PE-Cy5 (eBioscience, San Diego, CA), anti-c-kit/CD117-APC (eBioscience), anti-sca-1-PE-Cy7 (eBioscience), anti-T1/ST2-PE (R&D Systems, Minneapolis, MN) and anti-IL-17RB (R&D Systems) conjugated with AF750. Cells were fixed, subjected to flow cytometry and analyzed on a FACSAria II (BD Biosciences, San Jose, CA). Data were collected using FACSDiva software (BD Biosciences) and analyzed using FlowJo software (Tree Star, Ashland, OR). For analysis of intracellular IL-13, fresh aliquots of lung mince were stimulated for 5 h with cell stimulation cocktail (40.5 μM phorbol 12-myristate 13-acetate, 670 μM ionomycin, 5.3 mM brefeldin A, 1 mM monensin, eBioscience), Cells were then

stained for live/dead and surface markers, fixed, permeabilized and incubated with anti-mouse IL-13 clone eBio13A (eBioscience). Cells were analyzed with the FACSAria II.

Fluorescence-activated cell sorting of ILC2s. Lineage-negative CD25 and CD127 double-positive ILC2s or lineage-negative CD25 and CD127 double-negative cells were sorted at 9000 cells/200 µl into 96 well plates and stimulated with media, IL-25 (20 ng/ml), IL-2 (50 ng/ml) + IL-25 (20 ng/ml) or PMA + ionomycin for 3 days. To visualize ILC2s, cells were stained with Diff-Quick (Dade Behring, Newark, DE).

63 **TABLE E1.** qPCR primers.

64

Gene name	*Forward primer (5'->3')*	*Reverse primer (3'->5')*
GAPDH	GTC GGT GTG AAC GGA TTT G	GTC GTT GAT GGC AAC AAT CTC
Gob5	CTG TCT TCC TCT TGA TCC TCC A	CGT GGT CTA TGG CGA TGA CG
IFN-g	TGG CTG TTT CTG GCT GTT AC	TCC ACA TCT ATG CCA CTT GAG TT
IL-12p40	CTC CTG GTT TGC CAT CGT TT	GGG AGT CCA GTC CAC CTC TA
IL-13	CCT GGC TCT TGC TTG CGT	GGT CTT GTG TGA TGT TGC TCA
IL-17RB	ACC TTC CGG CGG CAA ATG GAC	GCA TTG GGG ATG TTA TGG GCG CT
IL-25	ACA GGG ACT TGA ATC GGG TC	TGG TAA AGT GGG ACG GAG TTG
IL-33	GGC TGC ATG CCA AGG ACA AGG	AAG GCC TGT TCC GGA GGC GA
IL-4	GGT CTC AAC CCC CAG CTA GT	GCC GAT GAT CTC TCT CAA GTG AT
IL-5	CTC TGT TGA CAA GCA ATG AGA CG	TCT TCA GTA TGT CTA GCC CCT G
Mub5b	GAG CAG TGG CTA TGT GAA AAT CAG	CAG GGC GCT GTC TTC TTC AT
Muc5ac	AAA GAC ACC AGT AGT CAC TCA GCA A	CTG GGA AGT CAG TGT CAA ACC
TNF-a	ATG CAC CAC CAT CAA GGA CTC AA	ACC ACT CTC CCT TTG CAG AAC TC

65

66

FIG E1. Viral copy number in RV-infected neonatal and adult mice. Six-day-old and eight week-old mice were inoculated with sham or RV intranasally. At specified times, lungs were harvested for analysis. Viral copy number was analyzed by qPCR. Shown are individual data, medians and interquartile range for each time point.

FIG E2. Persistent expression of mucus-related gene expression in 8 week-old mice infected with RV. Gene expression of Muc5ac, Muc5b, Gob5, and IL-13 was analyzed with quantitative PCR. * $P < 0.05$ versus sham (unpaired t-test).

FIG E3. Effect of RV infection on the expression of IL-25 and IL-33. Six-day-old neonatal BALB/c mice and eight-week-old mature mice were inoculated with sham or RV. Whole lung gene expression of IL-33 was measured 1-7 days after infection with quantitative PCR. *$P <$ 0.01 versus sham (unpaired t-test).

FIG E4. Effect of low-dosage RV infection in the induction of IL-25 and IFN-γ. Six-day-old neonatal BALB/c mice were inoculated with sham, or RV (normal dosage), or RV (10-fold lower dosage). Whole lung gene expression of IL-25 and IFN-γ mRNA was measured one day after infection with quantitative PCR. *$P < 0.05$ versus sham (unpaired t-test).

FIG E5. Lineage-negative cells in immature and mature mice. Six-day-old neonatal BALB/c mice and eight-week-old mature mice were inoculated with sham or RV. Lungs were collected 14 days after infection. Cell suspensions were stained with a cocktail of lineage antibodies (CD3ε, TCRβ, B220/CD45R, Ter-119, Gr-1/Ly-6G/Ly-6C, CD11b, CD11c, F4/80, and FcεRIα) and subjected to flow cytometry. The percentage of lineage-negative live cells was calculated. †$P < 0.05$ versus neonates (unpaired t-test).

FIG E6. Gating strategy for sorting ILC2s. Six-day-old neonatal BALB/c mice were infected with RV. After 8 days, lungs were processed for cell sorting. To sort ILC2s, low FSC, low SSC, DAPI-negative live cells were gated and incubated with lineage cocktail antibodies (CD3ε, TCRβ, B220/CD45R, Ter-119, Gr-1/Ly-6G/Ly-6C, CD11b, CD11c, F4/80, and FcεRIα). Finally, CD25 and CD127 double positive cells were identified.

References

E1. Newcomb DC, Sajjan U, Nanua S, Jia Y, Goldsmith AM, Bentley JK, et al. Phosphatidylinositol 3-kinase is required for rhinovirus-induced airway epithelial cell interleukin-8 expression. J. Biol. Chem. 2005; 280:36952-61.

E2. Johnston SL, Tyrrell DAJ. Rhinoviruses. In: Lennette EH, Schmidt NJ, editors. Diagnostic Procedures for Viral, Rickettsial, and Chlamydial Infections. Washington D.C.: American Public Health Association; 1997. p. 553-63.

E3. Martin S, Casasnovas JM, Staunton DE, Springer TA. Efficient neutralization and disruption of rhinovirus by chimeric ICAM-1/immunoglobulin molecules. J. Virol. 1993; 67:3561-8.

E4. Schneider D, Hong JY, Popova AP, Bowman ER, Linn MJ, McLean AM, et al. Neonatal rhinovirus infection induces persistent mucous metaplasia and airways hyperresponsiveness J. Immunol. 2012; 188:2894-904.

E5. Schneider D, Hong JY, Bowman ER, Chung Y, Nagarkar DR, McHenry CL, et al. Macrophage/epithelial cell CCL2 contributes to rhinovirus-induced hyperresponsiveness and inflammation in a mouse model of allergic airways disease. Am J Physiol Lung Cell Mol Physiol 2013; 304:L162-9.

Figure E1

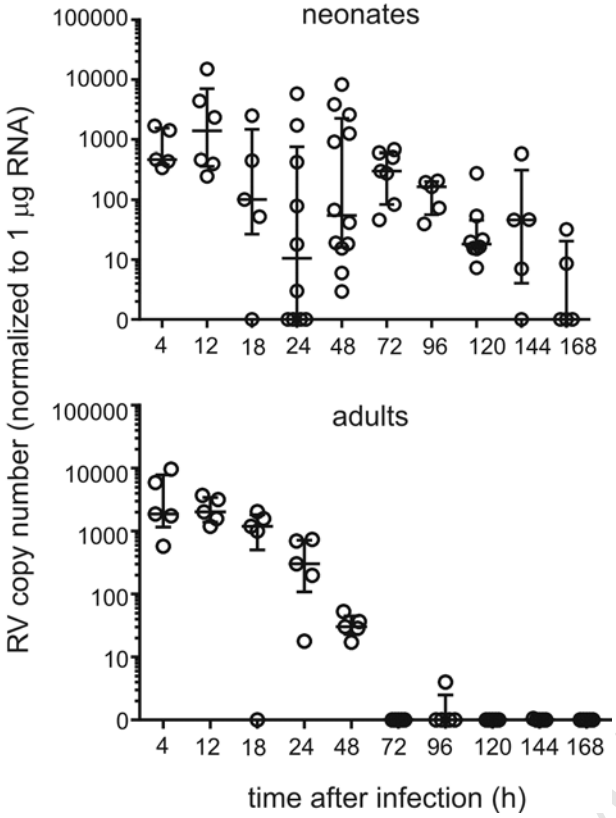

Figure E2

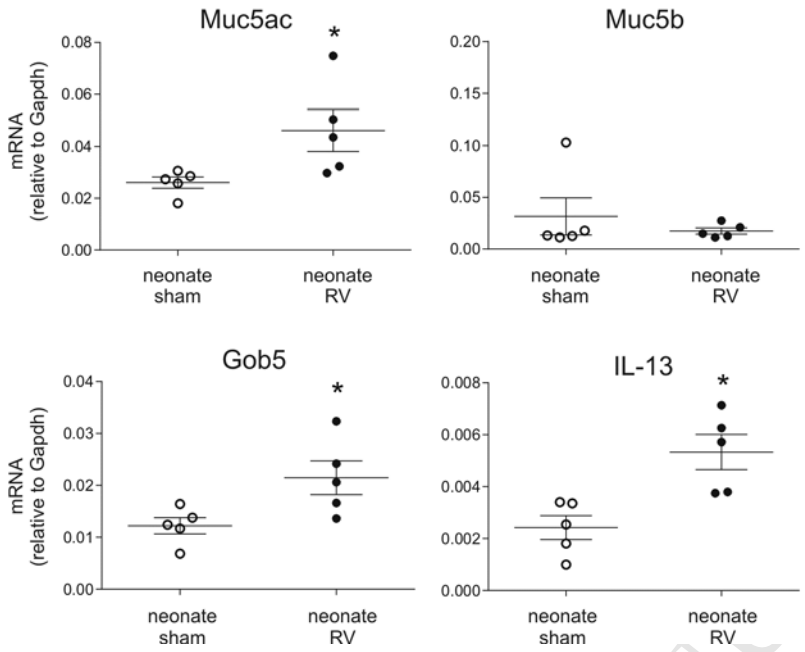

Figure E3

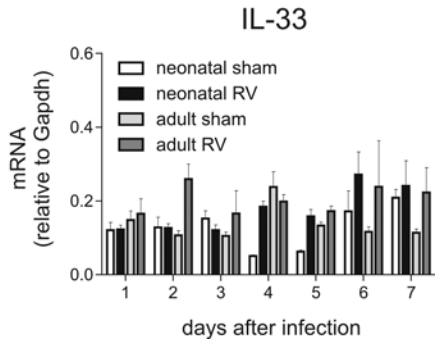

Figure E4

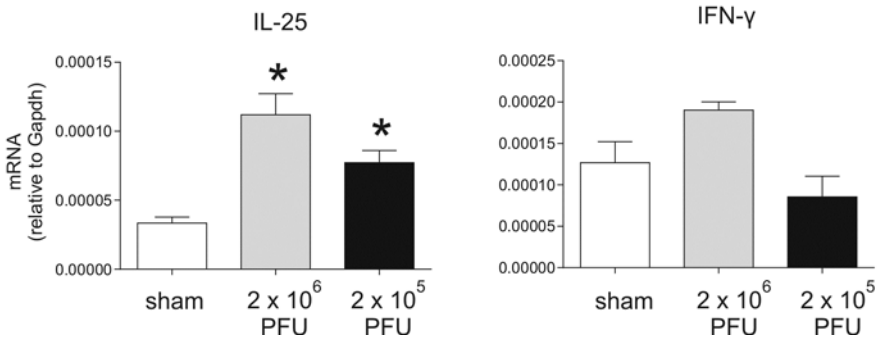

Figure E5

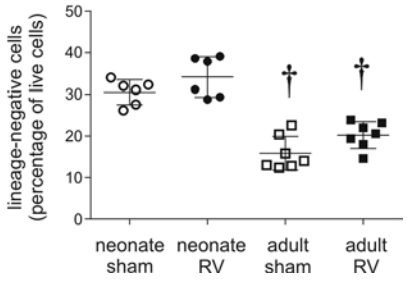

Figure E6